

# REGULARIZED ENERGY-DEPENDENT SOLAR FLARE HARD X-RAY SPECTRAL INDEX

Eduard P. KONTAR ([eduard@astro.gla.ac.uk](mailto:eduard@astro.gla.ac.uk))

*Department of Physics & Astronomy, University of Glasgow, G12 8QQ, United Kingdom*

Alexander L. MACKINNON ([alec@astro.gla.ac.uk](mailto:alec@astro.gla.ac.uk))

*Department of Adult and Continuing Education, University of Glasgow, G3 6NH, United Kingdom*

**Abstract.** The deduction from solar flare X-ray photon spectroscopic data of the energy dependent model-independent spectral index is considered as an inverse problem. Using the well developed regularization approach we analyze the energy dependency of spectral index for a high resolution energy spectrum provided by *Ramaty High Energy Solar Spectroscopic Imager* (RHESSI). The regularization technique produces much smoother derivatives while avoiding additional errors typical of finite differences. It is shown that observations imply a spectral index varying significantly with energy, in a way that also varies with time as the flare progresses. The implications of these findings are discussed in the solar flare context.

## 1. Introduction

Hard X-ray spectroscopy is considered to be an important tool for the study of high energy processes at the Sun (e.g. Brown, 1971; Lin and Hudson, 1976; Aschwanden, 2002), yielding vital, direct information on fast electron populations in flares. Specifically, the spatially integrated X-ray spectrum may be viewed as the convolution in electron energy of the bremsstrahlung cross-section and the mean electron flux in the source region (Brown, Emslie and Kontar, 2003). The functional form of the photon energy spectrum then contains information on the energy-dependence of the mean electron flux. This information may in turn be interpreted to bear on pictures of flare electron acceleration and propagation.

Even the earliest observations (e.g. Kane and Anderson, 1970) revealed the overall power-law form of the photon spectrum  $I(\epsilon)$  (photons  $\text{cm}^{-2} \text{s}^{-1} \text{keV}^{-1}$ ) above about 10 - 20 keV:  $I(\epsilon) \sim \epsilon^{-\gamma}$ , for some  $\gamma > 0$ . In the simplest possible (isotropic, non-relativistic) treatments of bremsstrahlung production, a power-law photon energy spectrum implies a source mean electron flux  $F(E)$  (electrons  $\text{s}^{-1}$ ) which is also a power-law in electron energy  $E$ . Further, simple assumptions about the post-acceleration propagation of electrons in the source (e.g. thin target, in which all electrons escape with negligible energy loss, or thick



© 2018 Kluwer Academic Publishers. Printed in the Netherlands.

target, in which all electrons stop completely in the source) then lead to  $F(E) \sim E^{-\delta}$ , with simple, linear relationships in each of the thick and thin target cases between  $\delta$  and  $\gamma$  (Brown, 1971).

A pure power-law form of  $F(E)$  would be an important clue to the nature of the acceleration process (Korchak, 1971). Power-law electron energy distributions are found commonly in nature and are a natural consequence of certain acceleration mechanisms (Miller et al, 1990; Petrosian et al., 1994). The distinctive feature of a power law, however, is the absence of any natural scale so it is probably true that any deviations from power-law behaviour give more decisive clues to the acceleration mechanism than the power law itself. Any such features would, of course, be reflected in deviations from power-law behaviour of  $I(\epsilon)$  - see Lin and Schwartz (1987) for an example. In particular,  $F(E)$  of power-law form only up to some maximum energy  $E_{max}$  would result in an  $I(\epsilon)$  which falls off more and steeply as  $\epsilon = E_{max}$  is approached.

Even for an accelerated pure power-law  $F(E)$ , electron transport and/or radiation physics may produce deviations from power-law behaviour in the observed spatially integrated photon spectrum. Anisotropy of the mean electron distribution combined with the directionality of bremsstrahlung emission for deka-keV electron energies would also have this effect, possibly with diagnostic potential for the source electron angular distribution (Massone et al, 2004). Compton back-scattering of photons from the photosphere (“X-ray albedo”) will also distort a power-law photon spectrum (Bai and Ramaty, 1978).

In a thick target, several physical processes may alter the analysis that leads to a power-law  $I(\epsilon)$  from a power-law  $F(E)$ , e.g. nonuniform ionisation (Brown, 1973; Kontar et al, 2003). As emitting electron energies approach thermal energies, the growing importance of velocity diffusion (as opposed to systematic mean slowing-down) will cause the mean electron distribution, and thus the photon spectrum, to deviate from a power law (Galloway et al., 2004). Noncollisional energy losses could have a wide variety of consequences for the photon spectrum (Brown and MacKinnon, 1985).

It seems clear that deviations from power-law  $I(\epsilon)$  hold significant diagnostic potential. We may define  $\gamma(\epsilon) = -(\epsilon/I)dI/d\epsilon$  as an energy-dependent spectral index, identically constant for a pure power-law  $I(\epsilon)$ , but likely to be informatively non-constant much of the time. Most earlier X-ray detectors had insufficient photon energy resolution to fully explore this potential, however, but we may now realistically aim to calculate  $\gamma(\epsilon)$  numerically from RHESSI (Lin et al, 2002) data.

With the simplest possible approximation (Kramers, 1923) to the bremsstrahlung cross-section we see further the relationship between the spectral index and the mean electron flux  $\bar{F}(E)$ , in particular il-

illustrating physically the connection between derivatives and an inverse problem. The photon flux is a convolution of the mean electron flux and the cross-section (Brown, 1971). Making Kramers' approximation we can write

$$I(\epsilon) = \frac{Q_0}{\epsilon} \int_{\epsilon}^{\infty} \frac{\bar{F}(E)}{E} dE \quad (1)$$

where  $Q_0$  is a constant. From the observed flux  $I(\epsilon)$  we need to obtain the mean electron flux. Differentiating both parts of (1) immediately leads us to the following

$$\bar{F}(E)|_{E=\epsilon} = \frac{\epsilon I(\epsilon)}{Q_0} [\gamma(\epsilon) - 1] \quad (2)$$

Since the photon flux is given from observations, Equation (2) shows that the spectral index uniquely determines the mean electron flux, at least in the limit that Kramers' approximation applies (Kramers, 1923).

Real data always come with noise, however, and numerical differentiation of data is a noise-amplifying process. Thus there is a need to establish reliable procedures for obtaining  $\gamma(\epsilon)$  (and more generally,  $dI/d\epsilon$ ) safely from data. Here we demonstrate that regularisation techniques (Groetsch, 1984; Hanke and Scherzer, 2001) can be applied for our purposes and yield such a robust procedure. The resulting smooth function may then be safely differentiated to obtain a best estimate of  $\gamma(\epsilon)$ . In Section 2 we give the formal demonstration of such an approach, in the process clarifying the sense in which this gives a “best” estimate. Section 3 applies this technique to obtain  $\gamma(\epsilon)$  from RHESSI data for the flare of 26 February, 2002 and study its time-dependence. Section 4 gives conclusions and discusses physical implications of the work carried out here.

## 2. Derivative as an inverse problem

Let us assume that we have a smooth function  $y(x)$  over the interval  $x_{01} \leq x \leq x_{02}$ . We have a finite sample  $y_i$  of measured values of this function, obtained over some grid  $x_{01} = x_0 < x_1 < \dots < x_i < \dots < x_n = x_{02}$  with mesh size  $\Delta x$ . The noisy data set has an error

$$|y_i - y(x_i)| \leq \delta y \quad (3)$$

where  $\delta y$  is an uncertainty of measurement.

We want to find the best smooth estimate of the derivative  $y'(x)$  using the given data set  $\forall x \in [x_{01}, x_{02}]$ . The two point finite difference estimate is readily available from the Cauchy expansion with the following bound

$$\left| \frac{y_{i+1} - y_i}{\Delta x} - y'(x_i) \right| \leq O(\Delta x + \delta y / \Delta x), \quad (4)$$

where the first and second terms in the right hand side represent consistency and propagation errors respectively (Groetsch, 1984). The first term in the right hand side comes from the discreteness of the data set, while the second is connected with the errors of the data  $\delta y$ .

Equation (4) explicitly shows that for decreasing  $\Delta x$  the error in the estimated derivative deteriorates rapidly, whereas for increasing  $\Delta x$  the error grows only linearly. The propagation error can be substantially suppressed by taking larger  $\Delta x$ , a procedure also known as regularization by coarse discretization. The extreme case of discretization corresponds to a linear fit. Obviously, this is far from desirable: although we have minimised the effects of error propagation we have only a single estimate of  $y'(x)$  across the whole of our range of  $x_i$ . On the contrary, we want to extract as much information as possible. The finite difference approach also leads to a non-smooth estimate of  $y'(x)$  - i.e. the resulting derivative is piecewise continuous. Note that the right-hand side of the Equation (4) reaches its minimum value which is  $O(\sqrt{\delta y})$  when  $\Delta x \sim \sqrt{\delta y}$ .

Let us now assume the existence of a function  $f(x)$ , which is a close approximation to the data set:

$$\frac{1}{n-1} \sum_{i=1}^n (y_i - f(x_i))^2 \leq (\delta y)^2, \quad (5)$$

Below we describe a detailed procedure for the construction of  $f(x)$ . We have to supplement this procedure with boundary conditions, the values of  $f(x)$  at two values of  $x$ . The values  $y_i$  at any two of the values  $x_i$  would suffice in principle. It might under some particular circumstances (e.g. suspected outliers) be appropriate to choose two of the interior points, but in what follows we simply choose the values at the endpoints, so that boundary conditions become:  $f(x_{01}) = y_0$ , and  $f(x_{02}) = y_n$ . Let us also assume that  $f(x)$  is a square integrable function over interval  $x \in [x_{01}, x_{02}]$ , so we can introduce a norm

$$\|f\| \equiv \left( \int_{x_{01}}^{x_{02}} f(x)^2 dx \right)^{1/2} \quad (6)$$

Hanke and Scherzer (2001) describe an optimal approach to constructing a smooth estimate of the derivative  $y'(x)$ . Following them,

we also require that the function  $f(x)$  has a smooth derivative, in the sense that

$$\|f''\| = \min \tag{7}$$

This means that we seek the function  $f(x)$  whose second derivative has the smallest norm. Roughly speaking, if we represent  $f(x)$  locally by the first two terms of its Taylor expansion,  $f''(x)$  gives an estimate of the error on  $f'(x)$  and minimising  $\|f''\|$  minimises the error in the resulting estimate for  $f'$ .

More specifically, let us estimate the error of our approximation if our basic conditions (5),(7) are met. The propagation error for the derivative  $f'$  can be estimated by considering the following norm

$$\|f' - y'\|^2 \leq \|f - y\| \|f'' - y''\| \tag{8}$$

where we integrated by parts and used the Cauchy-Schwarz inequality. The first factor in the right hand side is bounded by our requirement (5). The second factor is also limited as soon as  $\|f''\| \leq \|y''\|$ , which is true as long as equation (7) is satisfied. Now using the Minkowski inequality we arrive at the following result

$$|f'(x_i) - y'(x_i)| \leq O(\Delta x + \sqrt{\delta y}) \tag{9}$$

where we added consistency error in the same manner as in (4).

Comparing (9) and (4) we see the drastic difference. The former shows no growth for small values of  $\Delta x$ : fitting a suitably smooth function prior to estimating the derivative eliminates the uncertainty associated with estimates based on discrete bins. Moreover, the error (9) is bounded by the minimum in (4).

The result of this formal exercise can be formulated in terms of optimization (Hanke and Scherzer, 1998). Collecting our two requirements (5),(7) into a single equation, we require to minimise the functional:

$$\Phi(f) \equiv \frac{1}{n-1} \sum_{i=1}^{n-1} (y_i - \int_{x_0}^{x_i} f'(\xi) d\xi - y_0)^2 + \lambda \|f''(x)\|^2 \tag{10}$$

among all smooth functions  $f$  with  $f(\epsilon_{01}) = y(x_{01})$ ,  $f(x_{02}) = y(x_{02})$ , where  $\lambda$  is so that

$$\frac{1}{n-1} \sum_{i=1}^n (y_i - f_\lambda(x_i))^2 = (\delta y)^2 \tag{11}$$

where  $f_\lambda(x_i)$  is a solution of minimum problem (10). This is formally equivalent to an inverse problem and the solution method employed is well-known as Tikhonov regularization (Tikhonov, 1963). The equation (11) is also known as a discrepancy principle. It is interesting

to compare the problem (10) with the inversion of the photon data using second order regularization (see Kontar et al, 2004). The two problems are virtually identical. The only difference is the operator: the bremsstrahlung cross-section used in case of inversion of photon data, while our operator is an integrator. For the numerical implementation of this exercise, it is trivial to write the formal solution of the problem (10) using Generalized Singular Value Decomposition of our two operators: integrator and second order derivative (Kontar et al, 2004).

The solution of the problem (10,11) presents a regularized solution of the problem for  $f(x)$ . Figure 1 shows an example of this process applied to the function  $y(x) = \cos(x)$ , with a perturbation added in the form of random noise at the level of 1% of the value of  $y$ . The upper panel shows the actual data points generated in this way, together with the original function to emphasise how close the “data” points generated actually are. The lower panel shows values of the derivative calculated just by simple differencing of the data points, and the smooth curve generated by first regularising the data in the way described above. Judging from this, the derivative resulting from the regularization procedure is clearly much better. Compared to this, simple differencing of data with even this modest level of noise destructively affects the result.

### 3. Energy variation of spectral index in a solar flare

We defined the energy-dependent spectral index as a logarithmic derivative:  $\gamma(\epsilon) \equiv -d \ln I / d \ln \epsilon$ , where  $I(\epsilon)$  is an observed spectrum given as a data set  $I_i$  for every  $\epsilon_i$ . Choosing quantities  $x_i$  and  $y_i$  as follows

$$\ln(I_i) \rightarrow y_i, \quad \ln(\epsilon_i) \rightarrow x_i \quad (12)$$

we find our desired spectral index to be  $\gamma(\epsilon) = -f'(x)$ , where  $f(x)$  is determined from the measured values  $y_i$  as described in the previous section. We note here that since the bremsstrahlung photon spectrum is a convolution of cross-section and electron flux (Brown, Emslie and Kontar, 2003), logarithmic derivative of photon spectrum should always exist.

We now give a first, illustrative application using the RHESSI data from the GOES M-class flare that happened on February 26, 2002 around 10:27 UT (Figure 2). This event provides good photon count statistics while below the level of nonlinear features of the instrumental response such as pulse pile-up in the detectors (Smith et al, 2002). (These features are not fully understood and their details lie outside the scope of this paper.) Using standard software tools in SPEX we extracted the photon spectral flux (photons  $\text{keV}^{-1} \text{s}^{-1} \text{cm}^{-2}$ ) in the

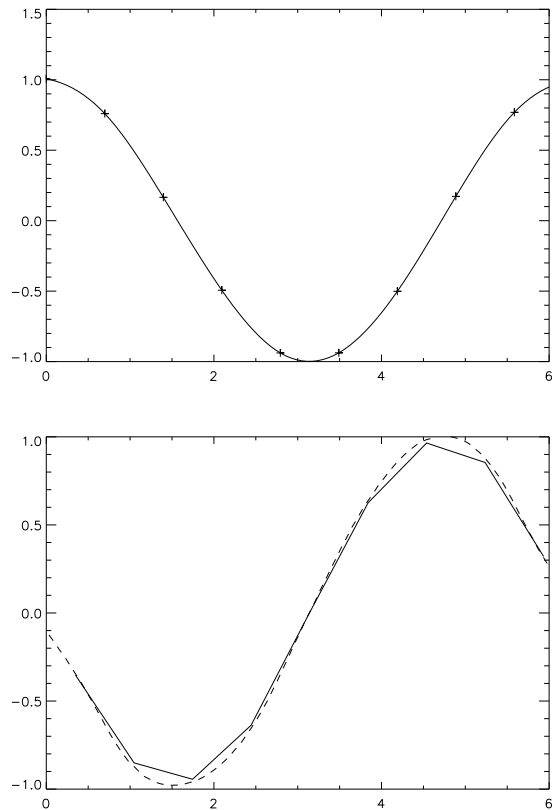


*Figure 1.* Numerical example. Function  $I(x) = \cos(x)$  (solid line) and data points (crosses) (upper panel) and its derivative (lower panel). Solid line is a regularized derivative for data points. The dash line shows the actual values of finite differences.

range above 10keV accumulated in seven front segments out of nine detectors. We omitted detectors 2 and 7 due to low operational energy resolution at the moment of the observation.

Figure 3 shows the spectrum of the solar flare observed by RHESSI on February 26, 2002 for the time interval 10:26:40-10:27:00 UT near at the peak of the flare. The lower panel shows the spectral index,  $\gamma(\epsilon)$ , calculated via the regularisation process described above. To construct error bars we first generated two further sets of “data”, one  $1\sigma$  above and one  $1\sigma$  below the original data points  $I(\epsilon_i)$ , where  $\sigma$  is the uncertainty on the photon spectrum. Then we applied the same regularisation procedure to these two new data sets. The resulting confidence interval in  $\gamma(\epsilon)$  allows us to highlight several features of interest, particularly in comparison with a other parametric descriptions of the

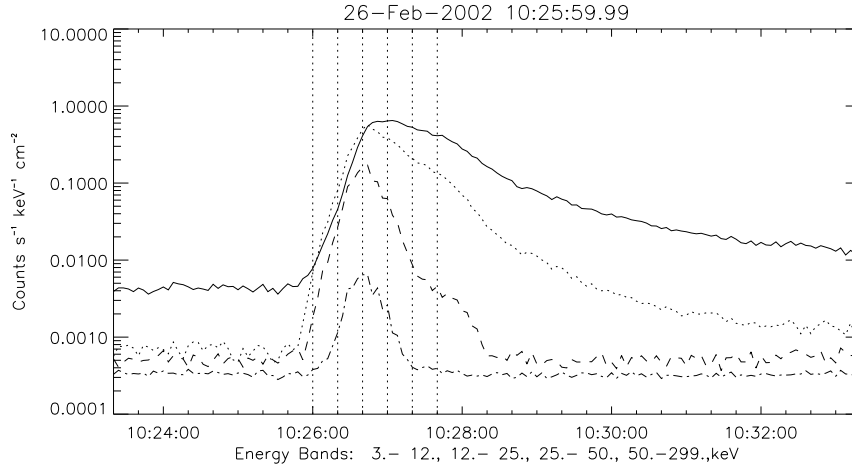


*Figure 2.* Temporal variation (4 seconds cadence) of the count rates in seven front RHESSI segments for the February 26, 2002 solar flare. The vertical lines show five 20 second selected accumulation intervals for spectral analysis.

spectrum and by implication its derivatives, for example an isothermal plus broken power-law spectral fit (Fig. 3) - cf. Holman et al. (2003).

Most immediately obvious (Fig. 3) is the nonconstancy of the spectral index within the energy range studied (10-100keV). At the lowest photon energies the regularized spectral index has a higher value than the index suggested by the isothermal plus power-law fit. This behaviour of spectral index may indicate X-ray emission from plasma with a range of temperatures. Similar suggestions of non-isothermality have been made by Piana et al. (2003), analyzing the mean electron flux spectrum deduced in the July 23 2002 flare and comparing to an isothermal and broken power-law fit (Holman et al, 2003). The regularized spectral index  $\gamma(\epsilon)$  also departs significantly from the broken power-law fit near the break energy 49 keV and above 70 keV. At the highest energies studied,  $\gamma(\epsilon)$  approaches 4, larger than the value found assuming a broken power-law. Above the thermal component, the spectral index grows approximately linearly with energy.

Figure 5 shows that for all time intervals the regularized spectral index shows a minimum, the position of which grows with time. There is a clear minimum for the first time interval at 10:26:00 UT near 17 keV, while at 10:27:20 UT the minimum is less clear and as high as 50 keV. Additionally, the spectral index varies less with energy as the flare progresses. The spectral index growths with energy by as much



as 3.0 for the first time interval, but it varies only by 0.1 for the last interval.

Earlier data from scintillation detectors established a relationship between spectral hardness (parametrised via a single value of  $\gamma$  derived from fitting across the available energy range) and total photon flux above some energy (Kane and Anderson, 1970). Specifically,  $\gamma$  obtained in this way is anti-correlated with total photon flux, so that the flare X-rays, viewed crudely, have the hardest spectrum when they are most intense. This “soft-hard-soft” spectral behaviour has been confirmed with RHESSI using ratios of photon flux in fairly broad bands (Fletcher and Hudson, 2002; Hudson and Farnik, 2002). Figure 5 shows the full, complex behaviour behind this simplified description. Values of  $\gamma(\epsilon)$  are indeed lowest, for any given  $\epsilon$ , around the peak of the event, but the decrease before and increase after this time do not occur at the same rate for all  $\epsilon$ . The flare starts with spectral index strongly dependent on energy, while a single power-law fit produces a mean spectral index which is a combination of small spectral index around 19 keV and relatively large  $\gamma(\epsilon)$  at 70 keV. In fact the minimum of the spectral index shows a tendency to grow as the flare progresses. Part of the transition from soft to hard spectra can thus be understood in terms of a reduction in the degree of variation with energy of  $\gamma(\epsilon)$  in the range 20 – 100 keV.

#### 4. Discussion

The illustration above shows vividly how far real spectra depart from the idealised power-law form. In this section we discuss some possible physical implications.

In standard models of hard X-ray production (e.g. Aschwanden, 2002) the X-ray emitting region is located well above the dense photosphere. X-rays emitted downwards will scatter on electrons of the dense layers of the solar atmosphere, finding their way back to an observer. The scattered flux, a function of the flare location and primary spectrum, may produce a detectable alteration of the net spectrum in the range 15-60 keV (Bai and Ramaty, 1978). Assuming the primary photon spectrum to be a simple power law (Bai and Ramaty, 1978) the photospheric albedo will peak at energies in the 20 - 40 keV range, with the reflected flux  $\approx 30 - 70\%$  of the primary flux. As a result, even if the primary spectrum is a pure power-law, the observed spectrum is flatter before the albedo peak energy and steeper above. This should be seen in the energy variation of the spectral index. For the February 26, 2002 flare, at heliocentric angle  $\approx 75^\circ$ ) and with photon spectral index

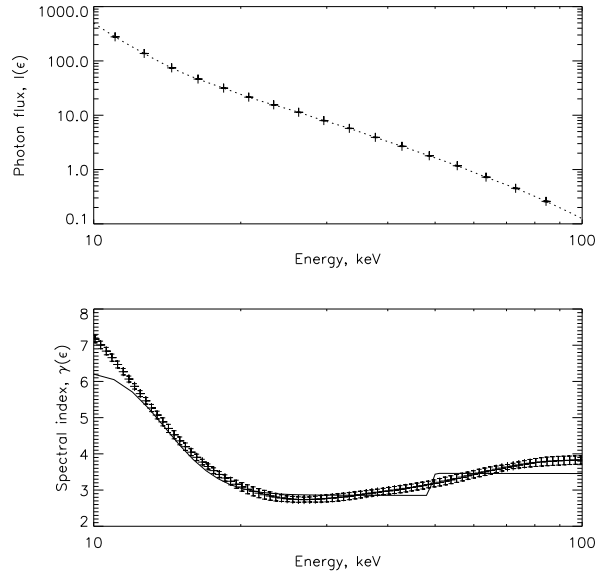


Figure 3. Spectrum of February 26, 2002 solar flare for 10:26:40-10:27:00 UT (upper panel crosses). The low panel shows the inferred spectral index with errors. The thick solid line presents the spectral index based on the isothermal plus broken power-law fit with  $\gamma_{low} = 2.8, \gamma_{upper} = 3.5$  with the break energy 49 keV.

$\approx 3$ , the results of Bai and Ramaty (1978) suggest that the albedo contribution to the observed spectrum will maximise near 35 keV, implying a lower spectral index below this energy and higher above. This tendency can indeed be seen in Figure (3). Nevertheless, albedo alone cannot account for the temporal variations shown in Figure 5, however - these must reflect properties of the primary X-ray spectrum, and thus of the emitting electron population.

Suppose that there is a high energy cut-off (or substantial softening) in the bremsstrahlung-emitting electron spectrum, at some energy  $E_{max}$ . For energies close to  $E_{max}$  the spectral index will be a growing function of  $\epsilon$ . Since the photon flux at a given energy is an integral over all electrons above this energy, the change of the spectral index due to a high energy cut-off can be seen at photon energies  $\epsilon$  well below  $E_{max}$  (Kontar et al, 2004). During the first time interval the variation with  $\epsilon$  of the spectral index is most significant, while the photon flux above 50 keV is very low (Figure 2). These facts together suggest a small number of electrons above 50 keV at this early time, while later in the flare the number of high energy electrons (above 100 keV) grows substantially. This is at the very least a plausible interpretation of

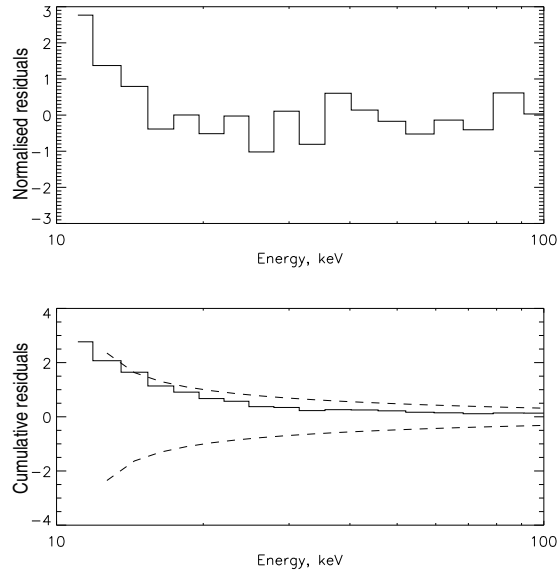


Figure 4. The residuals and the accumulated residuals for the time interval 10:26:40-10:27:00 UT (Fig. 3). The dash lines in the low panel present  $3\sigma$  level assuming residuals are statistically independent.

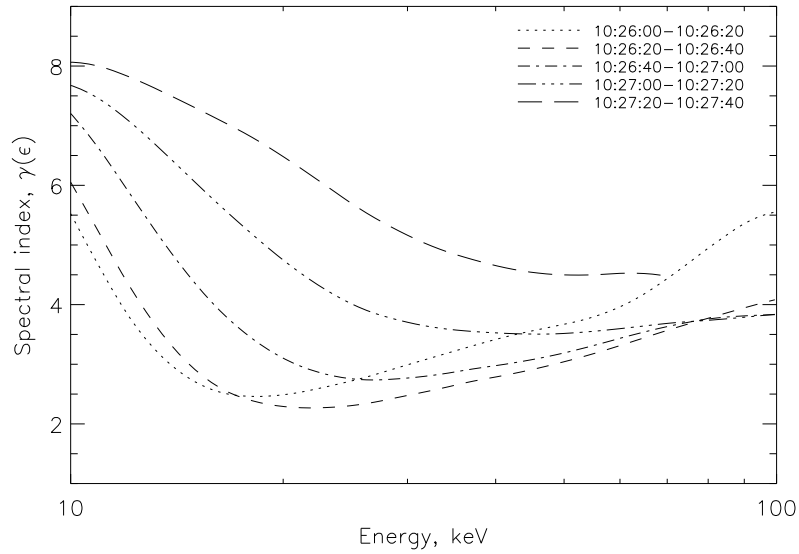


Figure 5. Temporal variation of energy dependent spectral index. Each line corresponds to one time interval.

the findings of Figure 5, suggesting that the “soft-hard-soft” pattern of spectral evolution really reflects changes in the highest electron energies present at different times.

A number of other physical processes may produce detectable variation in spectral index, even given an injected power-law electron energy distribution. For example, it was suggested (Brown, 1973; Kontar, Brown, and McArthur, 2002) that observed deviations from power-law can be interpreted as a manifestation of nonuniform target ionization. However, the possible variations of spectral index are unlikely to exceed 0.6 (Brown, Emslie, and Kontar, 2003). Moreover, the minimum of the spectral index if associated with chromospheric depth should show modest growth after the impulsive phase of the flare (Kontar et al, 2003), while the minimum of the spectral index shows no correlation with X-ray flux.

## 5. Conclusions

We have shown how best to estimate numerically the energy-dependent X-ray spectral index  $\gamma(\epsilon)$  from a set of observed photon fluxes at discrete energies, in a way that avoids the noise amplification of numerical differentiation. Formally the necessary procedure is equivalent to regularization. In consequence we have shown that the spectral index of at least one solar flare can have large variations with energy. The spectral index shows a clear minimum in the range 17-50 keV and the value of this minimum decreases as the flare progresses. The spectral index also tends towards energy-independence as the flare progresses, suggesting that something more like an ideal power-law photon spectrum is eventually attained. The origin of such variation can be connected with variability in the highest energy of the X-ray producing electrons. For later times the high energy cut-off is higher, thus producing a more uniform spectral index. This seems a simple, plausible explanation of the spectral behaviour found here; in particular it serves to illustrate the value of obtaining and studying  $\gamma(\epsilon)$ .

## ACKNOWLEDGMENT

The authors are thankful to John Brown, Brian Dennis, and Hugh Hudson for support, inspiring discussions and useful comments on the manuscript. This work is supported by a PPARC Rolling Grant.

## References

- Aschwanden, M.: 2002, *Space Science Reviews*, **101**, 1
- Bai, T., and Ramaty, R.:1978, *Astrophysical Journal*, **219**, 705
- Brown, J.C.: 1971, *Solar Physics*, **18**, 489
- Brown, J.C.: 1973, *Solar Physics*, **28**, 151
- Brown, J.C., Emslie, A.G., & Kontar, E.P.: 2003, *Astrophysical Journal*, **595**, L115
- Brown, J. C., and MacKinnon, A. L.: 1985, *Astrophysical Journal*, **292**, L31.
- Fletcher, L., Hudson, H. S.: 2002, *Solar Physics*, **210**, 317
- Galloway et al.: 2005, submitted to *Astronomy & Astrophysics*
- Groetsch, C.W.: 1984, *The Theory of Tikhonov Regularization for Fredholm Equations of the First Kind*, London: Pitman.
- Johns, C., & Lin, R. P.: 1992, *Solar Physics*, **137**, 121.
- Hanke, M. and Scherzer, O. 2001, *Amer. Math. Monthly* **108**, 512.
- Holman, G.D., Sui, L., Schwartz, R.A., Emslie, A.G.: 2003, *Astrophysical Journal*, **595**, L97
- Hudson, H. S., Farnik, F., 2002, *Proc. 10th European Solar Physics Meeting, 'Solar Variability: From Core to Outer Frontiers'*, Prague, Czech Republic, p. 261
- Kane, S.R., Anderson, K.A.: 1970, *Astrophysical Journal*, **162**, 1003.
- Kramers, H.A.: 1923, *Phil. Mag.*, **46**, 836
- Kontar, E.P., Brown, J.C. & McArthur, G.K.: 2002, *Solar Physics*, **210**, 419.
- Kontar, E.P., Brown, J.C., Emslie, A.G., Schwartz, R.A., Smith, D.M., Alexander, R.C.:2003, *Astrophysical Journal*, **595**, L123.
- Kontar, E.P., Piana, M., Massone, A.M., Emslie, A.G., and Brown, J.C.: 2004, *Solar Physics*, **225**, 293.
- Kontar, E.P., Emslie, A.G., Piana, M., Massone, A.M., and Brown, J.C.: 2005, *Solar Physics*, **226**, 317.
- Korchak, A.A.:1971, *Solar Physics*, **18**, 284.
- Lin, R.P., et. al.: 2002, *Solar Physics*, **210**, 3.
- Lin, R.P., and Hudson, H.S.: 1976, *Solar Physics*, **50**, 153.
- Lin, R.P.; Schwartz, R.A.:1987, *Astrophysical Journal*, **312**, 462.
- Massone, A.M., Emslie, A.G., Kontar, E.P., Piana, M., Prato, M., and Brown, J.C.: 2004, *Astrophysical Journal*, **613**, 1233.
- Miller, J.A., Guessoum, N., and Ramaty, R.: 1990, *Astrophysical Journal*, **361**, 701.
- Petrosian, V., McTiernan, J.M., and Marschhauser, H.:1994, *Astrophysical Journal*, **434**, 747.
- Piana, M., Massone, A.M., Kontar, E.P., Emslie, A. G., Brown, J.C., Schwartz, R.A.: 2003, *Astrophysical Journal* **595**, L127
- Smith, D.M. et al.:2002, *Solar Physics*, **210**, 33.
- Tikhonov, A. N. 1963, *Soviet Math. Dokl.*, **4**, 1035